Viscoelastic and Geometrically Nonlinear Behavior of Laminated Cylindrical Shells

Soo-Yong Lee* and Jungsun Park**

(Received May 6, 1999)

A viscoelastic and geometrically nonlinear finite element analysis is performed to investigate the stress relaxation and deflection of a laminated cylindrical shell under thermal loading. Incremental viscoelastic constitutive equations are derived to predict the stress relaxation. The finite element program is developed using a 3-D degenerated shell element, the first order shear deformation theory and the updated Lagrangian formulation. The viscoelastic and geometrically nonlinear analysis is executed for laminated shells with cross-ply and angle-ply stacking sequences, and its results are compared with those obtained from geometrically linear and viscoelastic analyses. The numerical results show that viscoelasticity and geometrical nonlinearity affect on the deflections and stresses of laminated cylindrical shells.

Key Words : Viscoelastic Analysis, Stress Relaxation, Laminated Cylindrical Shell, Nonlinear Finite Element Analysis

1. Introduction

To predict viscoelastic behavior of composite structures during the past decade, a number of viscoelastic analyses have been developed based on Schapery's viscoelasticity model (1967). Tuttle and Brinson (1986) developed a numerical procedure for predicting nonlinear viscoelastic response of laminated composites based on classical lamination theory. Henriksen (1984) developed a two dimensional finite element analysis for nonlinear viscoelastic behavior of an isotropic material. Roy and Reddy (1988) presented a similar analysis including large displacement and moisture diffusion. Lin and Hwang (1989) developed a two dimensional finite element analysis to study the linear viscoelastic response of anisotropic materials. Lin and Yi (1991) presented a similar analysis for generalized plane strain conditions. White and Hahn (1991) developed a process model for the investigation of viscoelastic residual stress development in laminates during cure processing and validated the model by the intermittent cure of unsymmetric cross-ply laminates in which curing induced residual curvatures were measured. Kennedy and Wang (1994) presented a three dimensional finite element analysis treating the nonlinear viscoelastic response of laminated composites. Kim (1996) introduced a viscoelastic constitutive equation depending on degree of cure and temperature by performing stress relaxation tests and investigated the residual stresses of Hercules AS4/3501-6 composite during the cure by analyzing two dimensional and axisymmetric problems.

The objective of this research is to investigate the viscoelastic and geometrically nonlinear behavior of the laminated cylindrical shell subjected to thermal loading. The viscoelastic finite element formulation will be developed on the basis of 3-D degenerated shell element and the first order shear deformation theory, and using the updated Lagrangian method. By analyzing the laminated cylindrical shells with orthotropic and angle-ply stacking sequences, the effect of viscoelasticity and geometrical nonlinearity on the defection and stress relaxation of the shell will be examined and the numerical results will be also compared with those of the elastic and

* Department of Aeronautical & Mechanical Engineering, Hankuk Aviation University.
** Department of Aerospace Engineering, Hankuk Aviation University.

geometrically nonlinear, the viscoelastic and geometrically linear, and the elastic and geometrically linear analyses.

2. Viscoelastic Constitutive Equation

Viscoelastic constitutive equations to predict the relaxation of stresses induced in composite shells by elevating temperature can be expressed by the following hereditary integral (Flaggs and Crossman, 1981 and Lin and Hwang, 1989) :

$$\mathbf{S}=\int_0^t \mathbf{C}(T,\ t-\tau)\frac{\partial \bar{\mathbf{E}}}{\partial \tau}d\tau \tag{1}$$

$$\bar{\mathbf{E}}=\mathbf{E}-\boldsymbol{\alpha}\Delta T \tag{2}$$

where $\mathbf{S}$ and $\mathbf{E}$ represent the second Piola-Kirchhoff stress tensor and the Green-Lagrange strain tensor, respectively. $\mathbf{C}$ and $\boldsymbol{\alpha}$ represent relaxation modulus and thermal expansion coefficient tensors, respectively. ΔT indicates the changes in temperature. t denotes time and τ is a dummy variable for integration. Assuming that a composite material is thermo-rheologically simple and then using a temperature-dependent reduced time, Eq. (1) can be expressed in the following form:

$$\mathbf{S}=\int_0^t \mathbf{C}(T_o,\ \xi^t-\xi^\tau)\frac{\partial \bar{\mathbf{E}}}{\partial \tau}d\tau \tag{3}$$

where T_o indicates the reference temperature and ξ represent the reduced time defined as

$$\xi^t=\int_0^t \frac{ds}{a_T[T(s)]},\quad \xi^\tau=\int_0^\tau \frac{ds}{a_T[T(s)]} \tag{4}$$

where a_T represents a shift factor expressed as a function of the temperature. Because generalized Maxwell models consisting of negative exponential functions are known as good approximations for the response of viscoelastic materials, the time-dependent relaxation modulus tensor $\mathbf{C}$ in Eq. (3) can be expressed in a finite exponential series of the form:

$$\mathbf{C}(\xi)=\mathbf{C}^\infty+\mathbf{C}^*\sum_{m=1}^{N}\mathbf{W}_m\exp\left(-\frac{\xi}{\tau_m}\right) \tag{5}$$

where $\mathbf{C}^\infty$ represents a fully relaxed modulus tensor and $\mathbf{C}^*=\mathbf{C}^u-\mathbf{C}^\infty$ where $\mathbf{C}^u$ represents an unrelaxed modulus tensor. τ_m and $\mathbf{W}_m$ are relaxation times and weighting factors, respectively. All parameters described above are determined from a viscoelastic experiment. Substituting Eq. (5) into Eq. (3), the viscoelastic constitutive equation is written as

$$\mathbf{S}^t=\int_0^t\left[\mathbf{C}^\infty+\mathbf{C}_0^*\sum_{m=1}^{N}\mathbf{W}_m\exp\left(-\frac{\xi^t-\xi^\tau}{\tau_m}\right)\right]\frac{\partial \bar{\mathbf{E}}}{\partial \tau}d\tau \tag{6}$$

We will now proceed to simplify the hereditary integral appearing in the constitutive equation in the manner proposed by Henriksen(1984) and used by Kennedy and Wang(1994), and derive a recursive formula that the solution at current time $t+\Delta t$ can be obtained using the solution known at the previous time t. First of all, at current time $t+\Delta t$, Eq. (6) can be rewritten as follows.

$$\mathbf{S}^{t+\Delta t}=\mathbf{C}^\infty\int_0^{t+\Delta t}\frac{\partial \bar{\mathbf{E}}}{\partial \tau}d\tau + \mathbf{C}^*\sum_{m=1}^{N}\mathbf{W}_m\int_0^{t+\Delta t}\exp\left(-\frac{\xi^{t+\Delta t}-\xi^\tau}{\tau_m}\right)\frac{\partial \bar{\mathbf{E}}}{\partial \tau}d\tau \tag{7}$$

Now let us define an equation as follows

$$\mathbf{S}_m^t=\mathbf{C}^*\mathbf{W}_m\int_0^t\exp\left(-\frac{\xi^t-\xi^\tau}{\tau_m}\right)\frac{\partial \bar{\mathbf{E}}}{\partial \tau}d\tau \tag{8}$$

and then the second integral in Eq. (7) at time $t+\Delta t$ can be defined as below.

$$\mathbf{S}_m^{t+\Delta t}=\mathbf{C}^*\mathbf{W}_m\int_0^{t+\Delta t}\exp\left(-\frac{\xi^{t+\Delta t}-\xi^\tau}{\tau_m}\right)\frac{\partial \bar{\mathbf{E}}}{\partial \tau}d\tau \tag{9}$$

This can be written in two parts as follows.

$$\mathbf{S}_m^{t+\Delta t}=\mathbf{C}^*\mathbf{W}_m\int_0^{t}\exp\left(-\frac{\xi^{t+\Delta t}-\xi^\tau}{\tau_m}\right)\frac{\partial \bar{\mathbf{E}}}{\partial \tau}d\tau + \mathbf{C}^*\mathbf{W}_m\int_0^{t+\Delta t}\exp\left(-\frac{\xi^{t+\Delta t}-\xi^\tau}{\tau_m}\right)\frac{\partial \bar{\mathbf{E}}}{\partial \tau}d\tau \tag{10}$$

For a sufficiently small time increment Δt, the reduced time at time $t+\Delta t$ can be expressed as

$$\xi^{t+\Delta t}=\xi^t+\Delta\xi^{t+\Delta t} \tag{11}$$

and the increment in the reduced time $\Delta\xi$ is defined as

$$\Delta\xi^{t+\Delta t}=\int_t^{t+\Delta t}\frac{ds}{a_T} \tag{12}$$

By assuming that the temperature is constant during the small time interval Δt, Eq. (12) can be approximated as

$$\Delta\xi^{t+\Delta t}=\frac{\Delta t}{a_T} \tag{13}$$

Using Eqs. (8) and (11), the first integral in Eq. (10) is expressed as

$$I_1=C^*W_m\int_0^t \exp(-\frac{\xi^{t+\Delta t}-\xi^\tau}{\tau_m})\frac{\partial\bar{E}}{\partial\tau}d\tau$$
$$=\exp(-\frac{\Delta\xi^{t+\Delta t}}{\tau_m})C^*W_m\int_0^t \exp(-\frac{\xi^t-\xi^\tau}{\tau_m})\frac{\partial\bar{E}}{\partial\tau}d\tau$$
$$=\exp(-\frac{\Delta\xi^{t+\Delta t}}{\tau_m})S_m^t \quad (14)$$

In order to solve the second integral in Eq. (9), let us assume that the change in the strain is constant in an interval of $t<\tau<t+\Delta t$. Namely,

$$\frac{\partial\bar{E}}{\partial\tau}\cong\frac{\bar{E}^{t+\Delta t}-\bar{E}^t}{\Delta t}=\text{constant} \quad (15)$$

Using Eqs. (13) and (15), and assuming that moduli and weighting factors are constant for Δt, the second integral in Eq. (10) can be derived as follows.

$$I_2=C^*W_m\int_t^{t+\Delta t}\exp(-\frac{\xi^{t+\Delta t}-\xi^\tau}{\tau_m})\frac{\partial\bar{E}}{\partial\tau}d\tau$$
$$\cong\frac{\bar{E}^{t+\Delta t}-\bar{E}^t}{\Delta t}C^*W_m\exp(-\frac{\xi^{t-\Delta t}}{\tau_m})\int_t^{t+\Delta t}\exp(\frac{\xi^\tau}{\tau_m})d\tau$$
$$=\frac{\bar{E}^{t+\Delta t}-\bar{E}^t}{\Delta t}C^*W_m\exp(-\frac{\xi^{t+\Delta t}}{\tau_m})\int_{\xi^t}^{\xi^{t+\Delta t}}\exp(\frac{\xi^\tau}{\tau_m})a_T d\xi \quad (16)$$

Integrating this equation gives

$$I_2=C^*W_m\frac{\tau_m}{\Delta\xi^{t+\Delta t}}\left[1-\exp(-\frac{\Delta\xi^{t+\Delta t}}{\tau_m})\right](\bar{E}^{t+\Delta t}-\bar{E}^t)$$
$$=C^*\Gamma_m^{t+\Delta t}\Delta\bar{E}^{t+\Delta t} \quad (17)$$

where $\Gamma_m^{t+\Delta t}$ and $\Delta\bar{E}^{t+\Delta t}$ are defined as

$$\Gamma_m^{t+\Delta t}=W_m\frac{\tau_m}{\Delta\xi^{t+\Delta t}}\left[1-\exp(-\frac{\Delta\xi^{t+\Delta t}}{\tau_m})\right] \quad (18)$$
$$\Delta\bar{E}^{t+\Delta t}=\bar{E}^{t+\Delta t}-\bar{E}^t \quad (19)$$

Therefore, substituting Eqs. (14) and (17) into Eq. (10) gives

$$S_m^{t+\Delta t}=\exp(-\frac{\Delta\xi^{t+\Delta t}}{\tau_m})S_m^t+\Gamma_m^{t+\Delta t}C^*\Delta\bar{E}^{t+\Delta t} \quad (20)$$

where the initial values of Γ_m^o and S_m^o at time $t=0$ are 1 and 0, respectively. From a computational point of view, Eq. (20) is much easier to deal with than Eq. (9) because Eq. (20) requires a knowledge of quantities at the previous time t, while Eq. (9) requires a knowledge of quantities over the complete history of the response of the material. Substitution of Eq. (20) into Eq. (7) leads to

$$S^{t+\Delta t}=C^\infty\int_0^{t+\Delta t}\frac{\partial\bar{E}}{\partial\tau}d\tau+\sum_{m=1}^N S_m^{t+\Delta t}$$
$$=C^\infty\int_0^{t+\Delta t}\frac{\partial\bar{E}}{\partial\tau}d\tau+\sum_{m=1}^N\exp(-\frac{\Delta\xi^{t+\Delta t}}{\tau_m})S_m^t$$
$$+\sum_{m=1}^N\Gamma_m^{t-\Delta t}C^*\Delta\bar{E}^{t+\Delta t} \quad (21)$$

Similarly, the stresses at time t can be expressed as

$$S^t=C^\infty\int_0^t\frac{\partial\bar{E}}{\partial\tau}d\tau+\sum_{m=1}^N S_m^t \quad (22)$$

By subtracting Eq. (22) from Eq. (21) and using Eq. (15), incremental stresses during the time interval Δt can be obtained as follows.

$$\Delta S^{t+\Delta t}=S^{t+\Delta t}-S^t$$
$$=\left[C^\infty+\sum_{m=1}^N\Gamma_m^{t+\Delta t}C^*\right]\Delta\bar{E}^{t+\Delta t}$$
$$+\sum_{m=1}^N\left[\exp(-\frac{\Delta\xi^{t+\Delta t}}{\tau_m})-1\right]S_m^t \quad (23)$$

This is the viscoelastic constitutive equation that represents the relationship of incremental stresses and strains during the small time step Δt. The stresses $S_m{}^t$ can be recursively calculated by Eq. (20). For the sake of simplicity, Eq. (23) can be written in the symbolic form as follows.

$$\Delta S^{t+\Delta t}=C^{t+\Delta t}\Delta\bar{E}^{t+\Delta t}+H^{t+\Delta t}$$
$$=C^{t+\Delta t}(\Delta E^{t+\Delta t}-\alpha\Delta T^{t+\Delta t})+H^{t+\Delta t} \quad (24)$$

where **C** and **H** are called time-dependent stiffness and hereditary stress tensors, respectively, which are defined as

$$C^{t+\Delta t}=C^\infty+\sum_{m=1}^N\Gamma_m^{t+\Delta t}C^* \quad (25)$$
$$H^{t+\Delta t}=\sum_{m=1}^N\left[\exp(-\frac{\Delta\xi^{t+\Delta t}}{\tau_m})-1\right]S_m^t \quad (26)$$

3. Viscoelastic and Geometrically Nonlinear Finite Element Formulation

The principle of virtual work corresponding to time $t+\Delta t$ with respect to an undeformed configuration ($t=0$) is expressed as

$$\int_{V^o}\delta(E^{t+\Delta t})^T S^{t+\Delta t}dV^o=\delta W^{t+\Delta t} \quad (27)$$

where the superscript **T** means transpose. V^o represents the volume at the undeformed configuration, and δW is the external virtual work defined as

$$\delta W^{t+\Delta t}=\int_{A^{t+\Delta t}}\delta(u^{t+\Delta t})^T f_s^{t+\Delta t}dA^{t+\Delta t}$$

$$+\int_{V^{t+\Delta t}}\delta(\mathbf{u}^{t+\Delta t})^{T}\mathbf{f}_{b}^{t+\Delta t}dV^{t+\Delta t} \quad (28)$$

where $\mathbf{u}$, $\mathbf{f}_s$, and $\mathbf{f}_b$ represent displacement, surface traction, and body force vectors, respectively, and $\mathbf{A}$ represent the area. If the variation is taken about the configuration at time t, the following equations are derived.

$$\mathbf{S}^{t+\Delta t}=\mathbf{S}^{t}+\Delta\mathbf{S}^{t+\Delta t}=\sigma^{t}+\Delta\mathbf{S}^{t+\Delta t} \quad (29)$$

$$\delta\mathbf{E}^{t+\Delta t}=\delta(\mathbf{E}^{t}+\Delta\mathbf{E}^{t+\Delta t})=\delta(\Delta\mathbf{E}^{t+\Delta t}) \quad (30)$$

$$\delta\mathbf{u}^{t+\Delta t}=\delta(\mathbf{u}^{t}+\Delta\mathbf{u}^{t+\Delta t})=\delta(\Delta\mathbf{u}^{t+\Delta t}) \quad (31)$$

where σ is the Cauchy stress tensor. The Cauchy stress tensor relating to time $t+\Delta t$ is obtained by using the following equation.

$$\sigma^{t+\Delta t}=\frac{1}{\det(\mathbf{F}^{t+\Delta t})}\mathbf{F}^{t+\Delta t}\,\mathbf{S}^{t+\Delta t}(\mathbf{F}^{t+\Delta t})^{T} \quad (32)$$

where $\mathbf{F}$ represents the deformation gradient tensor calculated with respect to the configuration at time t. Substituting Eqs. (29) ~ (31) into Eqs. (27) and (28) and using the updated Lagrangian formulation with the reference configuration at time t, Eqs. (27) and (28) are rewritten as

$$\int_{V^{t}}\delta(\Delta\mathbf{E}^{t+\Delta t})^{T}(\sigma^{t}+\Delta\mathbf{S}^{t+\Delta t})dV^{t}=\delta\mathbf{W}^{t+\Delta t} \quad (33)$$

$$\delta\mathbf{W}^{t+\Delta t}=\int_{A^{t+\Delta t}}\delta(\Delta\mathbf{u}^{t+\Delta t})^{T}\mathbf{f}_{s}^{t+\Delta t}dA^{t+\Delta t}+\int_{V^{t+\Delta t}}\delta(\Delta\mathbf{u}^{t+\Delta t})^{T}\mathbf{f}_{b}^{t+\Delta t}dV^{t+\Delta t} \quad (34)$$

The incremental Green-Lagrangian strain tensor can be divided in two parts.

$$\Delta\mathbf{E}^{t+\Delta t}=\Delta\mathbf{e}^{t+\Delta t}+\Delta\eta^{t+\Delta t} \quad (35)$$

where $\Delta\mathbf{e}$ and $\Delta\eta$ represent incremental linear and nonlinear strain tensors, respectively. Substitution of Eq. (35) into Eq. (33) leads to

$$\int_{V}\delta\mathbf{E}^{T}\Delta\mathbf{S}\,dV+\int_{V}\delta\eta^{T}\,\sigma dV=\delta\mathbf{W}-\int_{V}\delta\mathbf{e}^{T}\,\sigma dV \quad (36)$$

where the superscripts indicating time are dropped hereafter for the sake of convenience and the following contracted notations were used in Eq. (36).

$$\delta(\Delta\mathbf{E}^{t+\Delta t})=\delta\mathbf{E},\ \delta(\Delta\mathbf{e}^{t+\Delta t})=\delta\mathbf{e},\ \text{and}\ \delta(\Delta\eta^{t+\Delta t})=\delta\eta \quad (37)$$

Substitution of the incremental viscoelastic constitutive relation given by Eq. (24) into Eq. (36) leads to

$$\int_{V}\delta\mathbf{E}^{T}\,\mathbf{C}\Delta\mathbf{E}dV+\int_{V}\delta\eta^{T}(\sigma-\mathbf{C}\,\alpha\Delta\mathrm{T}+\mathbf{H})dV=\delta\mathbf{W}-\int_{V}\delta\mathbf{e}^{T}(\sigma-\mathbf{C}\,\alpha\Delta\mathrm{T}+\mathbf{H})dV \quad (38)$$

Linearization of Eq. (38) with the approximation $\delta\mathbf{E}^{T}\mathbf{C}\Delta\mathbf{E}=\delta\mathbf{e}^{T}\mathbf{C}\Delta\mathbf{e}$ leads to

$$\int_{V}\delta\mathbf{e}^{T}\,\mathbf{C}\Delta\mathbf{e}dV+\int_{V}\delta\eta^{T}(\sigma-\mathbf{C}\,\alpha\Delta\mathrm{T}+\mathbf{H})dV=\delta\mathbf{W}-\int_{V}\delta\mathbf{e}^{T}(\sigma-\mathbf{C}\,\alpha\Delta\mathrm{T}+\mathbf{H})dV \quad (39)$$

On the basis of 3-D degenerated shell element and the first order shear deformation theory (Chao and Reddy, 1984 and Panda and Natarajan, 1981), the incremental displacement vector $\Delta\mathbf{u}$ in an isoparametric element with P nodal points is defined as (Bathe, 1982)

$$\Delta\mathbf{u}=\sum_{k=1}^{P}N^{k}(\xi,\eta)\Delta\bar{\mathbf{u}}^{k}+\frac{1}{2}\sum_{k=1}^{P}N^{k}(\xi,\eta)t^{k}\zeta\Delta V^{k} \quad (40)$$

where ξ, η, ζ denote the local coordinates of the element and $\Delta\bar{\mathbf{u}}^{k}$, N^{k}, t^{k} represent the incremental displacement vector, shape function and thickness at nodal point k of the element, respectively. ΔV^{k} represents, at nodal point k, the difference between unit vectors normal to the shell mid-surface at time $t+\Delta t$ and at time t, that is, $\mathbf{V}_{t+\Delta t}^{k}-\mathbf{V}_{t}^{k}$. Expressing the incremental displacement and strain vectors by a function of the nodal displacement vector gives

$$\Delta\mathbf{u}=\mathbf{N}\,\Delta\bar{\mathbf{u}},\ \Delta\mathbf{e}=\mathbf{B}_{L}\,\Delta\bar{\mathbf{u}},\ \text{and}\ \Delta\eta=\mathbf{B}_{NL}\,\Delta\bar{\mathbf{u}} \quad (41)$$

where $\mathbf{N}$, $\mathbf{B}_L$ and $\mathbf{B}_{NL}$ represent the shape function matrix, the linear and nonlinear displacement-strain matrices, respectively (Bathe, 1982). By substituting Eq. (41) into Eq. (39) and using a modified Newton-Raphson iterative method, the viscoelastic and geometrically nonlinear finite element formulation is summarized as

$$(\mathbf{K}_{L}^{t+\Delta t}+\mathbf{K}_{NL}^{t+\Delta t})\Delta\bar{\mathbf{u}}_{(i)}^{t+\Delta t}=\mathbf{R}^{t+\Delta t}-\mathbf{F}_{(i-1)}^{t+\Delta t} \quad (42)$$

where the time-dependent stiffness matrix $\mathbf{K}$ and the force vectors $\mathbf{R}$ and $\mathbf{F}$ are given by

$$\mathbf{K}_{L}^{t+\Delta t}=\int_{V^{t}}\mathbf{B}_{L}^{T}\,\mathbf{C}^{t+\Delta t}\,\mathbf{B}_{L}dV^{t} \quad (43)$$

$$\mathbf{K}_{NL}^{t+\Delta t}=\int_{V^{t}}\mathbf{B}_{NL}^{T}(\sigma^{t+\Delta t}-\mathbf{C}^{t+\Delta t}\alpha\Delta\mathrm{T}^{t+\Delta t}+\mathbf{H}^{t+\Delta t})\,\mathbf{B}_{NL}dV^{t} \quad (44)$$

$$\mathbf{R}^{t+\Delta t}=\int_{A^{t+\Delta t}}\mathbf{N}^{T}\mathbf{f}_{s}^{t+\Delta t}dA^{t+\Delta t}+\int_{V^{t+\Delta t}}\mathbf{N}^{T}\mathbf{f}_{b}^{t+\Delta t}dV^{t+\Delta t}$$

$$+\int_{V_t} B_L^T(C^{t+\Delta t}\alpha\Delta T^{t+\Delta t}-H^{t+\Delta t})dV^t \quad (45)$$

$$F_{(i-1)}^{t+\Delta t}=\int_{V_{(i-1)}^{t+\Delta t}} B_L^T\sigma_{(i-1)}^{t+\Delta t}\,dV^{t+\Delta t} \quad (46)$$

where the parentheses in Eqs. (44) and (45) are written in the matrix and vector forms, respectively. Note that the modulus C given by Eq. (28) was recalculated with the assumption that the stress normal to the shell surface is zero. After solving Eq. (42) with boundary conditions for each iteration, the nodal displacement vector during the time (or load) step Δt is updated as follows.

$$\bar{u}_{(i)}^{t+\Delta t}=\bar{u}_{(i-1)}^{t}+\Delta\bar{u}_{(i)}^{t+\Delta t}\ ;\ \bar{u}_{(0)}^{t+\Delta t}=\bar{u}^t \quad (47)$$

The iterative procedure in Eq. (42) continues until the convergence condition presented below is satisfied at each time step.

$$\frac{\|\Delta\bar{u}_{(i)}^{t+\Delta t}\|}{\|\bar{u}_{(i)}^{t+\Delta t}\|}\le \text{Error} \quad (48)$$

After one time step is finished, the strains and stresses are updated by substituting Eq. (47) into Eq. (41) and using Eqs. (24) and (29)$\sim$(32), and then Eq. (20) is updated for the next time step.

5. Numerical Results and Discussion

Viscoelastic data and material properties of Hercules AS4/3501-6 composite used in the analysis are presented in Tables 1 and 2. The values given in Table 2 are used to calculate the modulus C given by Eq. (5). Since stress relaxation in the direction of a fiber can be negligible, the components C_{11}, C_{12}, and C_{13} related to the fiber direction are assumed to be linearly elastic. The fully relaxed modulus C^{∞} is experimentally determined by 1/7 of the unrelaxed modulus C^{u} (Kim, 1996). The element used for the finite element analysis is a 8-node degenerated shell element with five degrees of freedom per node and $2\times2\times2$ Gauss integration points are used at each layer of the element to prevent shear locking. Because the accuracy of numerical results depends on the time step Δt, the finite element analyses are executed for three time steps $\Delta t=10$ sec, 30 sec, and 1 min for the purpose of examining the convergence of numerical solutions and it is found that there is no big difference between them. Therefore, to save computational time, the time step $\Delta t=1$ min is used for the numerical analyses presented below. The value of the error in Eq. (48) used for the geometrically nonlinear analysis is 1×10^{-4}.

Table 1 Relaxation times and weighting factors.

m	τ_m(min)	W_m
1	2.922137e+1	0.0591334
2	2.921437e+3	0.0661225
3	1.82448e+5	0.0826896
4	1.1031059e+7	0.112314
5	2.8305395e+8	0.154121
6	7.9432822e+9	0.2618288
7	1.953424e+11	0.1835594
8	3.3150756e+12	0.0486939
9	4.9174856e+14	0.0262258

Table 2 Mechanical properties of AS4/3501-6 used in calculations.

Young's modulus, E_{11}	125.38 GPa
Young's modulus, E_{22}	8.1 GPa
Young's modulus, E_{33}	8.1 GPa
Shear modulus, G_{12}	4.1 GPa
Shear modulus, G_{13}	4.1 GPa
Shear modulus, G_{23}	2.75 GPa
Poisson's ratio, ν_{12}	0.25
Poisson's ratio, ν_{13}	0.25
Poisson's ratio, ν_{23}	0.47
Thermal expansion coeff., α_{11}	0.5e-6 1/℃
Thermal expansion coeff., α_{22}	35.3e-6 1/℃
Thermal expansion coeff., α_{33}	35.3e-6 1/℃

In order to verify the finite element program developed in this study, two examples are studied. First of all, a model as shown in Fig. 1 is selected for the comparison of the viscoelastic analysis. Both ends of a laminated plate are clamped and the length, width, and thickness of the plate are 100 mm, 10 mm, and 2 mm, respectively, and fiber

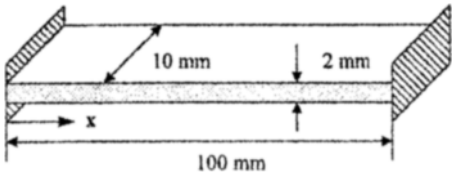

Fig. 1 Geometry of the clamped laminated plate

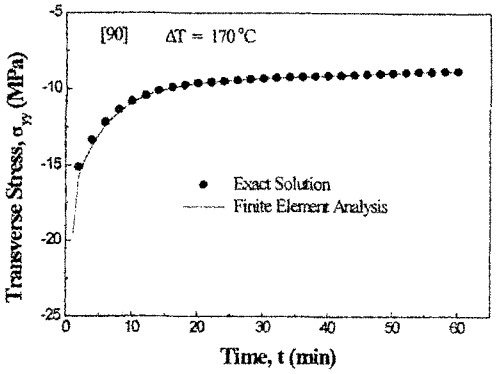

Fig. 2 Comparison of the finite element analysis with the exact solution for the transverse stress in the laminated plate

orientation is 90° normal to the x-axis in Fig. 1. If the temperature is given as $\Delta T\, h(t)$ where $h(t)$ is a unit step function, the exact solution for a one dimensional problem can be obtained from Eq. (6). The total strain in Eq. (2) is given as zero because the ends of the plate are clamped. By substituting Eqs. (2) and (4) into Eq. (6) and integrating it, an one dimensional exact solution with small deformation can be expressed as

$$\sigma_2^I=\left[E_{22}^{\infty}+E_{22}^{*}\sum_{m=1}^{N}W_m\exp\left(-\frac{t}{\tau_m a_T}\right)\right](-\alpha_{22}\Delta T) \quad (49)$$

where the subscript 2 represents the direction normal to the fiber orientation and E represents Young's modulus. In Eq. (49), σ_2 indicates the stress corresponding to the small deformation. For the viscoelastic finite element analysis, the plate shown in Fig. 1 is divided by 10 meshes in length and 2 meshes in width. Total number of elements is 20. When the temperature change ΔT is 170°C, two results obtained from Eq. (49) and the finite element analysis are compared in Fig. 2. The result of the finite element analysis is calculated at the center of the plate. The results agree well each other as shown in Fig. 2.

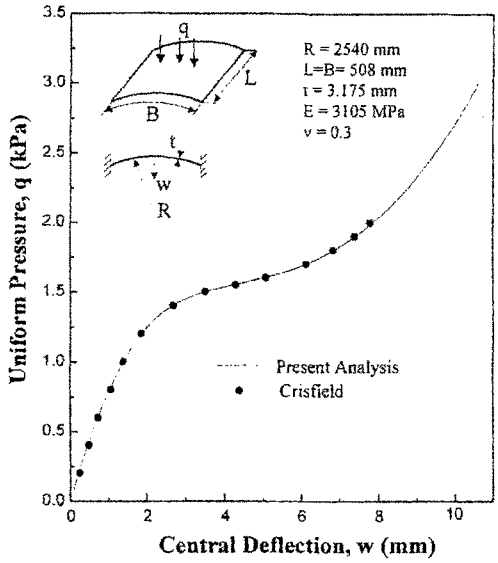

Fig. 3 The fully clamped cylindrical shell under uniform pressure loading

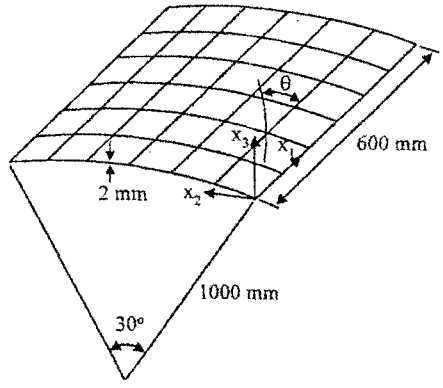

Fig. 4 Geometry of the laminated cylindrical shell

Secondly, the geometrically nonlinear analysis is performed for an isotropic cylindrical shell under an uniform pressure loading and compared with the result of Crisfield(1981) as shown in Fig. 3. All edges of the shell are clamped and a quarter of the shell is analyzed using a 5×5 element mesh. As shown in Fig. 3, two results also agree well. Hence, validation of the finite element program developed in this paper is accomplished.

To predict viscoelastic and geometrically nonlinear behavior of a laminated cylindrical shell under thermal loading, the shell as shown in Fig. 4 is presented. The radius, length and thickness of

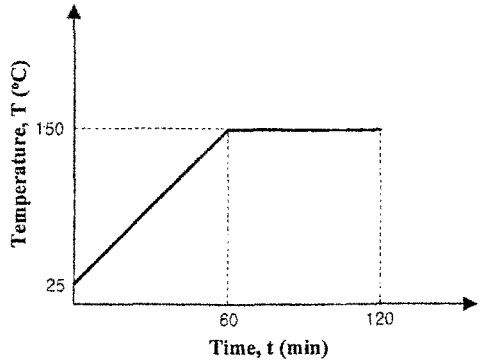

Fig. 5 Temperature used in calculations

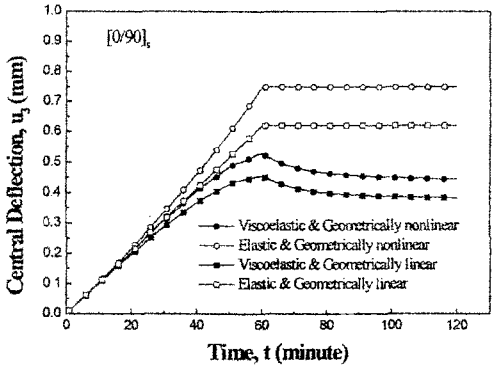

Fig. 6 Comparison of deflections at the center of the laminated cylindrical shell under thermal loading

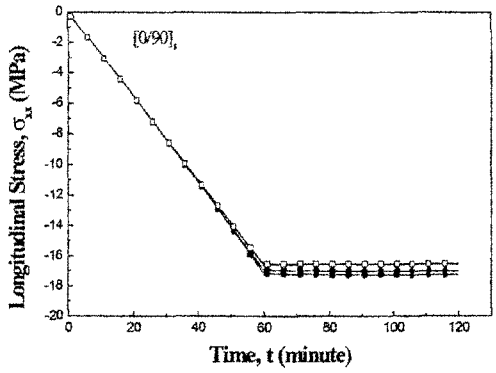

Fig. 7 Comparison of logitudinal stresses at the center of the laminated cylindricall shell under thermal loading

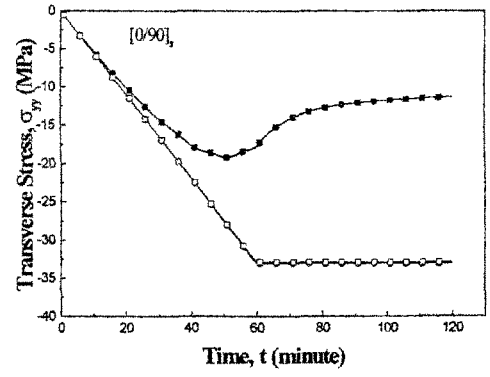

Fig. 8 Comparison of transverse normal stresses at the center of the laminated cylindrical shell under thermal loading

the shell are 1000 mm, 600 mm and 2 mm, respectively. The laminated shell consists of 4 plies. All four edges of the shell are clamped and temperature distribution is assumed to be uniform. The shell is analyzed using a 6×6 element mesh with 113 nodes.

In order to investigate the viscoelastic and geometrically nonlinear behavior of the laminated cylindrical shell under the thermal loading as shown in Fig. 5, the finite element analysis was performed and compared with three results of the elastic and geometrically nonlinear, the viscoelastic and geometrically linear, and the elastic and geometrically linear analyses in Figs. 6~12.

Figures 6~8 show the results for a $[0/90]_s$ laminated shell where a positive fiber orientation θ is shown in Fig. 4. Deflections are calculated at the center of the shell. The stresses presented in the figures are the on-axis Cauchy stresses calculated at the first ply (0°) and at the center of the shell. As shown in Fig. 6, the central deflections are quite different for the various types of the analyses mentioned above. The geometrically nonlinear and viscoelastic effects on the deflections are opposite each other. The first one tends to increase the central deflections, whereas the second does to decrease. Figure 8 shows that the viscoelastic effect is significant for the transverse stress.

Figures 9~12 show the numerical results for a $[30/-30]_s$ laminated shell. The deflections are calculated at the center of the shell. The on-axis stresses are also calculated at the first ply (30°) and at the center of the shell. The viscoelastic and geometrically nonlinear effects on the deflections presented in Fig. 9 are just opposite to the results in Fig. 6. As shown in Figs. 10~12, the viscoelas-

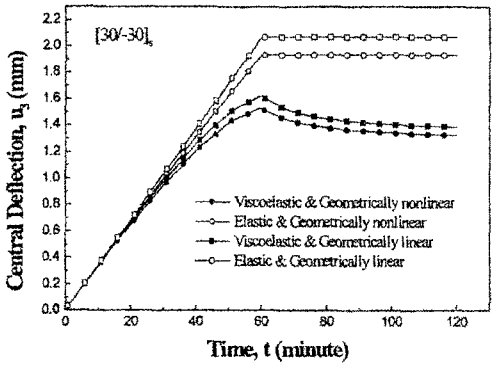

Fig. 9 Comparison of deflections at the center of the laminated cylindrical shell under thermal loading

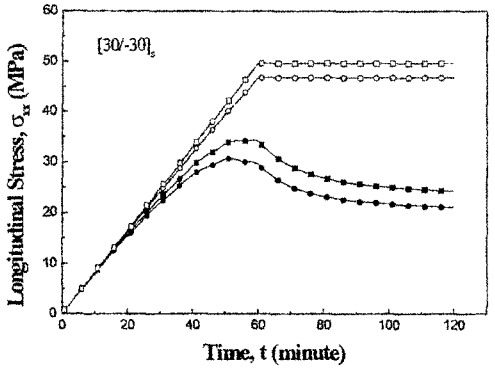

Fig. 10 Comparison of logitudinal stresses at the center of the laminated cylindrical shell under thermal loading

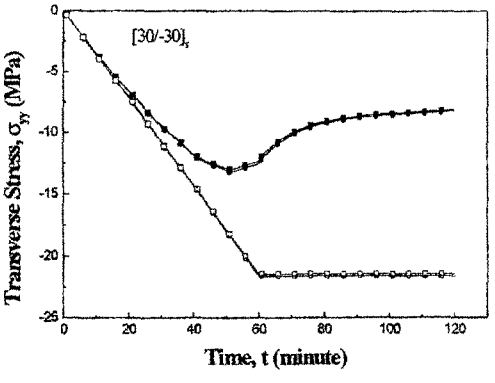

Fig. 11 Comparison of transverse normal stresses at the cnter of the laminated cylindrical shell under thermal loading

tic effect is significant for all the stresses and the geometrically nonlinear effect is significant for only the longitudinal stress.

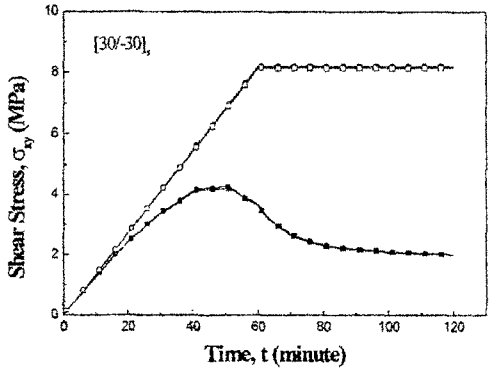

Fig. 12 Comparison of inplane shear stresses at the center of the laminated cylindrical shell under thermal loading

5. Conclusions

In this study, the viscoelastic and geometrically nonlinear finite element analysis has been performed to investigate the stress relaxation and deflection of the laminated cylindrical shell under the thermal loading. The incremental viscoelastic constitutive equations that can describe the stress relaxation is derived as a recursive formula used conveniently for numerical analysis. Using the 3-D degenerated shell element, the first order shear deformation theory and the updated Lagrangian formulation, the finite element program has been developed and verified by comparing with the one dimensional exact viscoelastic solution and the geometrically nonlinear solution provided by Crisfield (1981).

The viscoelastic and geometrically nonlinear finite element analysis has been performed for the laminated cylindrical shells with $[0/90]_s$ and $[30/-30]_s$ stacking sequences, and the results have been compared with those obtained from the elastic and geometrically nonlinear, the viscoelastic and geometrically linear, and the elastic and geometrically linear analyses. The numerical results show that the viscoelasticity and geometrical nonlinearity affect on the deflections and stresses of the shells.

References

Bathe, K. J., 1982, *Finite Element Procedures in Engineering Analysis*, Prentice Hall.

Chao, W. C. and Reddy, J. N., 1984, "Analysis of Laminated Composite Shells Using a Degenerated 3-D Element," *International Journal for Numerical Methods in Engineering*, Vol. 20, pp. 1991~2007.

Crisfield, M. A., 1981, "A Fast Incremental/Iterative Solution Procedure that handles Snap-Through," Computers and Structures, Vol. 13, pp. 55~62.

Flaggs, D. L. and Crossman, F. W., 1981, "Analysis of the Viscoelastic Response of Composite Laminates During Hygrothermal Exposure," *Journal of Composite Materials*, Vol. 15, pp. 21~40.

Henriksen, M., 1984, "Nonlinear Viscoelastic Stress Analysis- A Finite Element Approach," *Computers & Structures*, Vol. 18, pp. 133~139.

Kennedy, T. C. and Wang, M., 1994, "Three-Dimensional Nonlinear Viscoelastic Analysis of Laminated Composites," *Journal of Composite Materials*, Vol. 28, pp. 121~132.

Kim, Y. K., 1996, "Process-Induced Viscoelastic Residual Stress Analysis of Graphite-Epoxy Composite Structures," *Ph. D. Dissertation*, Department of Aeronautical and Astronautical Engineering, University of Illinois at Urbana-Champaign.

Lin, K. Y. and Hwang, I. H., 1989, "Thermo-Viscoelastic Analysis of Composite Materials," *Journal of Composite Materials*, Vol. 23, pp. 554~569.

Lin, K. Y. and Yi, S., 1991, "Analysis of Interlaminar Stresses in Viscoelastic Composites," *International Journal of Solids and Structures*, Vol. 27, pp. 929~945.

Panda, S. C. and Natarajan, R., 1981, "Analysis of Laminated Composite Shell Structures by Finite Element Method," *Computers & Structures*, Vol. 14, pp. 225~230.

Roy, S. and Reddy, J. N., 1988, "Finite Element Models of Viscoelasticity and Diffusion in Adhesively Bonded Joints," *International Journal for Numerical Methods in Engineering*, Vol. 26, pp. 2531~2546.

Schapery, R. A., 1967, "Stress Analysis of Viscoelastic Composite Materials," *Journal of Composite Materials*, Vol. 1, pp. 228~267.

Tuttle, M. E. and Brinson, H. F., 1986, "Prediction of the Long-Term Creep Compliance of General Composite Laminates," *Experimental Mechanics*, Vol. 26, pp. 89~102.

White, S. R. and Hahn, H. T., 1992, "Process Modelling of Composite Materials: Residual Stress Development during Cure. Part I. Model Formulation," *Journal of Composite Materials*, Vol. 26, pp. 2402~2422.